HHS Public Access

Author manuscript

Angew Chem Int Ed Engl. Author manuscript; available in PMC 2019 December 21.

Published in final edited form as:

Angew Chem Int Ed Engl. 2018 December 21; 57(52): 17069–17072. doi:10.1002/anie.201809865.

Segmental ^{13}C-labeling and Raman Microspectroscopy of α-Synuclein Amyloid Formation

Jessica D. Flynn[a], **Zhiping Jiang**[a], **Jennifer C. Lee**[*,a]

[a]National Heart, Lung, and Blood Institute, National Institutes of Health, Bethesda, MD 20892, United States

Abstract

Mapping conformational changes of α-synuclein (α-syn) from soluble, unstructured monomers to β-sheet-rich aggregates is crucial towards understanding amyloid formation. Here, we use Raman microspectroscopy to spatially resolve conformational heterogeneity of amyloid aggregates and monitor amyloid formation of segmentally ^{13}C-labeled α-syn in real-time. As the ^{13}C-isotope shifts the amide-I stretching frequency to lower energy, the ligated construct, $^{13}C_{1–86}{}^{12}C_{S87C-140}$-α-syn, exhibits two distinct bands allowing for simultaneous detection of secondary structural changes in N-terminal 1–86 and C-terminal 87–140 residues. The disordered-to-β-sheet conformational change is first observed for the N-terminal followed by the C-terminal region. Finally, Raman spectroscopic changes occurred prior to Thioflavin T fluorescence enhancement, indicating that the amide-I band is a superior probe of amyloid formation.

Graphical Abstract

Two peaks are better than one.

Native chemical ligation was used to segmentally label α-synuclein with ^{13}C. This labelling scheme results in two spectroscopically distinct amide-I bands that independently report on region-specific conformational changes of the protein backbone. The N-terminal region was seen to adopt β-sheet structure first in the formation of amyloid.

[*]Corresponding author leej4@mail.nih.gov.

Supporting information for this article is given via a link at the end of the document.

Experimental Section

Experimental details are available in the online supporting information.

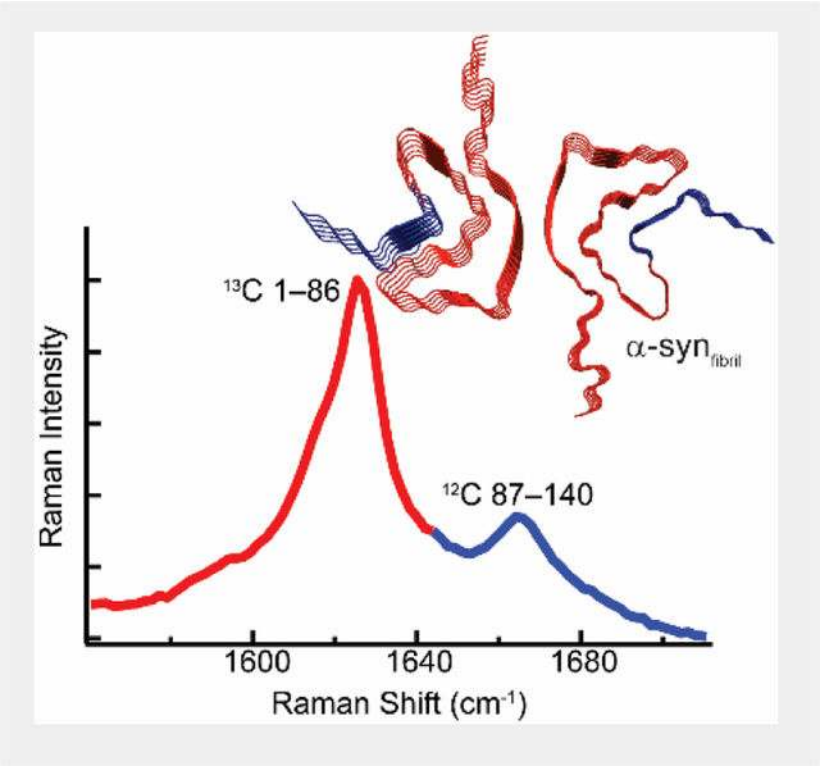

Keywords

kinetic intermediates; chemical ligation; aggregation; transmission electron microscopy; β-sheet

Parkinson's disease (PD) is a neurodegenerative disorder that results from the death of cells in the *substantia nigra* region of the brain.[1] A diagnostic hallmark of PD is the presence of intracellular brain inclusions, called Lewy bodies, which contain high amounts of α-synuclein (α-syn) amyloid fibrils, similar to the β-sheet-rich fibrils formed spontaneously by α-syn in vitro.[2] The primary sequence of α-syn is generally considered as three segments with distinct molecular characteristics. The N-terminal residues 1–89 are amphipathic and responsible for membrane binding, while most of the residues among 61–95 are nonpolar and hydrophobic, known as the NAC (non-amyloid β component) region critical for fibril formation.[3] The remaining C-terminal portion is highly charged with 15 carboxylic acids and removal of this region promotes rapid aggregation of α-syn.[4] Notably, α-syn C-terminal truncations are found inside Lewy bodies,[5] reaffirming a strong connection between α-syn aggregation propensity and PD. Consequently, understanding region-specific molecular details that influence α-syn aggregation is crucial in elucidating its role in disease.

Much effort has been previously invested in using site-specific fluorescent and nitroxide-spin probes to monitor α-syn fibril formation and structure.[6] Despite their utility in measuring conformational and local environmental changes, these studies lack the ability to directly yield secondary structural information. Raman spectroscopy is well-suited for this application because the amide-I band is spectroscopically distinct for an unstructured

polypeptide compared to a β-sheet-rich fibrillar aggregate (Figure S1), and therefore acts as direct reporter of protein secondary structure.[7] Further, its high chemical specificity and an insensitivity to aqueous background makes Raman spectroscopy particularly powerful for observing α-syn aggregation under aqueous conditions.[8] Here, we use Raman microspectroscopy and segmentally ^{13}C-labeled α-syn to spatially resolve conformational heterogeneity of amyloid aggregates and monitor amyloid formation of α-syn in real-time, providing region-specific structural details.

Using our previously published α-syn construct and native chemical ligation (NCL) protocol,[9] uniformly ^{13}C-labeled N-terminal residues 1–86 are covalently linked to the C-terminal ^{12}C-complement containing residues 87–140, referred to from here as $^{13}C_{1–86}{}^{12}C_{S87C–140}$ or ligated-α-syn (Figure 1A). This strategy generates region-specific Raman contrast within one α-syn protein and affords the ability to assign secondary structural changes to respective polypeptide regions. As the protease-resistant core of α-syn consists of residues 28–114,[8] both the ^{13}C- and ^{12}C-amide-I stretches will report on β-sheet formation during aggregation, with N-terminal region containing more of the amyloid core residues. Our approach is analogous to a previous 2D-IR study on segmental ^{13}C-labeled γD-crystallin fibrils;[10] however, to our knowledge, this is the first report of segmental ^{13}C-isotopic labeling used for Raman microspectroscopy.

The Raman spectrum of aggregated ligated-α-syn clearly shows the vibrational changes due to ^{13}C-isotopic labeling when compared to that of aggregated uniformly-labeled ^{12}C- and ^{13}C-α- syn (30 μM protein in 10 mM NaOAc, 100 mM NaCl, pH 5, incubated at 37 °C) (Figure 1B). For example, the carbonyl stretch of the peptide backbone (1666 cm^{-1}, blue curve) shifts to lower energies (1626 cm^{-1}, red curve). This decrease in amide-I frequency (40 cm^{-1}) is in accord with literature values.[11] In the ligated construct, we consequently observe two distinct amide-I peaks: ^{13}C=O and ^{12}C=O in the N- and C-terminal residues centered at 1626 and 1666 cm^{-1}, respectively.

The relative Raman intensity ratio of the ^{13}C:^{12}C amide-I peaks is 3:1 for ligated-α-syn, which is consistent with the expected ratio from the β-strand assignments based on solid-state NMR and cryoEM structures.[12] We also observe a large shift of the amide-III band (1230 cm^{-1} for ^{12}C) in the ligated-α-syn spectrum, suggesting this vibrational mode is strongly influenced by the N-terminal region polypeptide backbone. Interestingly, we see very little perturbation of the C-H deformation stretch (1450 cm^{-1}) of ligated-α-syn. This suggests the C-H deformation vibrational mode is due largely to the rocking motion of the hydrogens and is minimally perturbed by isotopic labeling. Figure 1C shows fibril morphologies for ligated-α-syn are indistinguishable to those formed by ^{13}C- and ^{12}C-α-syn, indicating chemical ligation is not perturbative to amyloid fibril formation.

At the nanoscopic-level, amyloid fibrils appear as thin filaments, tens of nanometers wide and up to several microns long (Figure 1C). At the microscopic-level, the morphologies of amyloid aggregates observed by brightfield microscopy are distinctly different from isolated fibrils imaged by TEM and offer a new perspective on α-syn aggregation. Figure 2A shows the rough morphology of an insoluble α-syn aggregate (780 μM protein in 10 mM NaOAc, 100 mM NaCl, pH 5, incubated at 37 °C). Spectra in Figure 2B, which correspond to the

spatial locations noted in the black outline in Figure 2A, show subtle differences in the peak intensities of the ^{13}C- and ^{12}C-amide-I bands, observed at 1626 cm^{-1} and 1669 cm^{-1}, respectively, indicative of structural variations. Additionally, second-derivative analysis (Figure 2C), which is used to determine spectral components and peak shifts,[13] shows the peak width and position of the ^{12}C amide-I (1669 cm^{-1}) vary more than the ^{13}C amide-I band (1626 cm^{-1}), suggesting a more heterogenous distribution of secondary structures in the C-terminal residues. This observation agrees with prior literature that this region is more disordered.[14] Furthermore, these structural differences suggest the C-terminal region is influencing fibril structure, which is well documented for α-syn.[15]

To observe secondary structural changes during amyloid formation, Raman spectra were measured for two independent ligated-α-syn aggregation reactions as a function of incubation time (*Run* 1 at 780 μM and Run 2 at 550 μM protein in 10 mM NaOAc, 100 mM NaCl, pH 5, incubated at 37 °C). For each time point, several Raman spectra were collected at independent spatial locations and averaged. The full sets of individual Raman spectra for each time point are shown in Figure S2 – S5. In Figure 3A, the Raman spectral evolution upon α-syn aggregation is shown as Raman difference spectra (t_n–t_0, where n = the indicated time point minus initial spectrum at time 0) for Run 1 (left) and Run 2 (right). Similar kinetic trends are observed for both runs. For the first 1.5–1.75 h of aggregation, few changes are seen in the spectral window 1525–1725 cm^{-1}, where the broad amide-I bands remain in relatively low intensity (Figure S2 and S4). As aggregation proceeds, the Raman signal increases and there is a positive change in the difference spectrum. At 3.25 h, a peak in the difference spectrum is now resolved for the ^{13}C-amide-I band in Run 1, signifying conformational changes within residues 1–86. We observe a similar peak at 3.5 h for Run 2. Beyond 4 h, the Raman signature of β-sheet secondary structure can now be seen for the ^{12}C-amide-I band, corresponding to the involvement of residues 87–140, and continues to increase for the ^{13}C-amide-I band. Interestingly, once β-sheet structure forms in the N-terminal region, the Raman peak at 1626 cm^{-1} gains intensity, but does not change in peak position. The ^{12}C-amide-I band, however, narrows as aggregation proceeds, suggesting that the C-terminal region is more dynamic and takes longer to become ordered compared to the N-terminal region.

The normalized average intensities of the ^{13}C-amide-I (1626 cm^{-1}), ^{12}C-amide-I (1669 cm^{-1}), and C-H deformation (1450 cm^{-1}, Figure S3 and S5) stretchs were also compared as a function of time (Figure 3B). From this analysis, we observe a lag phase for all peaks with no changes from 0 to 1.5 h. Interestingly, the intensities for ^{13}C- and ^{12}C-amide-I bands in Run 1 show local maxima at 2 h, suggestive of a kinetic intermediate, where there is more change for the C-terminal residues (*i.e.* ^{12}C=O peak). This intermediate is not evident in Run 2, likely due to the stochastic and heterogenous process of aggregation. To elucidate the nature of this intermediate would require further experiments in which a single aggregate is monitored *in situ* over time.

After 4 h, we see dramatic intensity gain for all monitored frequencies, due to rapid amyloid formation. When compared to a commonly used fluorophore, Thioflavin T (ThT), for detection of amyloids,[16] changes in the Raman spectrum precede ThT response, offering

early structural insights not available through this standard assay. This early structural sensitivity was also observed for ^{12}C-α-syn (Figure S8).

Importantly, by coupling our Raman spectrometer to an inverted microscope, we are able to spatially visualize and to interrogate individual aggregation events, which are obscured in bulk measurements. At 0 h, there are no observable aggregates by brightfield imaging or TEM (Figure 4A, top row). Correspondingly, the Raman spectrum measured at a single, spatial location shows a broad amide-I band with low signal intensity (Figure 4B, red curve), characteristic of soluble, ligated- α-syn. At 2h, small, round aggregates begin to appear in brightfield microscopy, while TEM images reveal only nanometer-scale amorphous aggregates (Figure 4A, middle row). Spectroscopically, the Raman signal of these small aggregates shows a narrowing in the ^{13}C-amide-I band, indicating the presence of β-sheet structure in the N-terminal residues (Figure 4B, green curve). The ^{12}C-amide-I band, however, remains broad, suggesting a disordered conformation in the C-terminal region, indicating that at early times, non-fibrillar intermediates contain β- sheet secondary content only in the N-terminal region. At 3.25 h, large aggregates with rough morphologies appear in brightfied microscopy, and a few, short fibrillar structures are now observed by TEM (Figure 4A, bottom row). Additionally, at 3.25 h, there is now a more prominent ^{12}C amide-I peak at the characteristic frequency for β-sheet structure along with a sharpened ^{13}C amide-I peak (Figure 4B, purple curve). This observation suggests that fibrils are populating only after 3.25 h and that β- sheet formation in both N- and C-terminal region is needed.

Taken together, our data highlight the strength of coupling the chemical specificity of Raman spectroscopy with the spatial resolution of a microscope to better understand the relationship between the microscopic and nanoscopic events of amyloid formation. We see the formation of insoluble aggregates, with β- sheet structure, preceeds filament formation (as observed by TEM) and enhanced ThT emission. Segmental ^{13}C-labeling allows us to directly identify that β-sheet structure first forms in the N-terminal region, followed by the C-terminal region of ligated-α- syn. Further, we see that within a single, microscopic aggregate, the C-terminal region is less uniform than the N-terminal region. From this work, we gain both molecular and mechanistic insights into α-syn amyloid formation and we anticipate this strategy will be broadly applicable to other studies of amyloid formation.

Supplementary Material

Refer to Web version on PubMed Central for supplementary material.

Acknowledgements

This work was supported by the Intramural Research Program at the NIH, NHLBI. Parts of this research was performed on instruments maintained by the NHLBI Electron Microscopy (TEM) and Biochemistry (LC-MS) Core Facilities.

References

[1]. Lees AJ, Hardy J, Revesz T, The Lancet 2009, 373, 2055–2066.
[2]. Chiti F, Dobson CM, Annu Rev Biochem 2006, 75, 333–366. [PubMed: 16756495]

[3]. a)Iwai A, Yoshimoto M, Masliah E, Saitoh T, Biochemistry 1995, 34, 10139–10145; [PubMed: 7640267] b)Giasson BI, Murray IVJ, Trojanowski JQ, Lee VM-Y, J Biol Chem 2001, 276, 2380–2386. [PubMed: 11060312]

[4]. a)Levitan K, Chereau D, Cohen SI, Knowles TP, Dobson CM, Fink AL, Anderson JP, Goldstein JM, Millhauser GL, J Mol Biol 2011, 411, 329–333; [PubMed: 21689664] b)Murray IVJ, Giasson BI, Quinn SM, Koppaka V, Axelsen PH, Ischiropoulos H, Trojanowski JQ, Lee VMY, Biochemistry 2003, 42, 8530–8540; [PubMed: 12859200] c)Hoyer W, Cherny D, Subramaniam V, Jovin TM, Biochemistry 2004, 43, 16233–16242. [PubMed: 15610017]

[5]. Baba M, Nakajo S, Tu PH, Tomita T, Nakaya K, Lee VM, Trojanowski JQ, Iwatsubo T, Am J Pathol 1998, 152, 879–884. [PubMed: 9546347]

[6]. a)Thirunavukkuarasu S, Jares-Erijman EA, Jovin TM, J Mol Biol 2008, 378, 1064–1073; [PubMed: 18433772] b)Yap TL, Pfefferkorn CM, Lee JC, Biochemistry 2011, 50, 1963–1965; [PubMed: 21338068] c)Dusa A, Kaylor J, Edridge S, Bodner N, Hong D-P, Fink AL, Biochemistry 2006, 45, 2752–2760; [PubMed: 16489768] d)Kaylor J, Bodner N, Edridge S, Yamin G, Hong D-P, Fink AL, J Mol Biol 2005, 353, 357–372; [PubMed: 16171820] e)Lee JC, Langen R, Hummel PA, Gray HB, Winkler JR, Proc Natl Acad Sci U S A 2004, 101, 16466–16471; [PubMed: 15536128] f)Ferreon AC, Gambin Y, Lemke EA, Deniz AA, Proc Natl Acad Sci U S A 2009, 106, 5645–5650; [PubMed: 19293380] g)Nath S, Meuvis J, Hendrix J, Carl SA, Engelborghs Y, Biophys J 2010, 98, 1302–1311; [PubMed: 20371330] h)Haney CM, Petersson EJ, Chem Commun 2018, 54, 833–836;i)Der-Sarkissian A, Jao CC, Chen J, Langen R, J Biol Chem 2003, 278, 37530–37535. [PubMed: 12815044]

[7]. a)Carey PR, Annu Rev Phys Chem 2006, 57, 527–554; [PubMed: 16599820] b)Flynn JD, Lee JC, Chem Commun 2018, 54, 6983–6986;c)Rygula A, Majzner K, Marzec KM, Kaczor A, Pilarczyk M, Baranska M, J Raman Spectrosc 2013, 44, 1061–1076.

[8]. Flynn JD, McGlinchey RP, Walker RL 3rd, Lee JC, J Biol Chem 2018, 293, 767–776. [PubMed: 29191831]

[9]. a)Jiang Z, Heinrich F, McGlinchey RP, Gruschus JM, Lee JC, J Phys Chem Lett 2017, 8, 29–34; [PubMed: 27936328] b)Ligation site at S87 was chosen to minimize side-chain perturbation and split the protein into peptide fragments suitable for E. coli experssion (1–86 and 87–140).

[10]. Moran SD, Woys AM, Buchanan LE, Bixby E, Decatur SM, Zanni MT, Proc Natl Acad Sci U S A 2012, 109, 3329–3334. [PubMed: 22328156]

[11]. Dong J, Wan Z-L, Chu Y-C, Nakagawa SN, Katsoyannis PG, Weiss MA, Carey PR, J Am Chem Soc 2001, 123, 7919–7920. [PubMed: 11493071]

[12]. a)Tuttle MD, Comellas G, Nieuwkoop AJ, Covell DJ, Berthold DA, Kloepper KD, Courtney JM, Kim JK, Barclay AM, Kendall A, Wan W, Stubbs G, Schwieters CD, Lee VM, George JM, Rienstra CM, Nat Struct Mol Biol 2016, 23, 409–415; [PubMed: 27018801] b)Guerrero-Ferreira R, Taylor NMI, Mona D, Ringler P, Lauer ME, Riek R, Britschgi M, Stahlberg H, eLife 2018, 7, e36402; [PubMed: 29969391] c)Li Y, Zhao C, Luo F, Liu Z, Gui X, Luo Z, Zhang X, Li D, Liu C, Li X, Cell Res 2018.

[13]. a)Balestrieri C, Colonna G, Giovane A, Irace G, Servillo L, Eur J Biochem 1978, 90, 433–440; [PubMed: 710441] b)Heino S, Byler DM, Biochem Biophys Res Commun 1983, 115, 391–397. [PubMed: 6615537]

[14]. Vilar M, Chou HT, Luhrs T, Maji SK, Riek-Loher D, Verel R, Manning G, Stahlberg H, Riek R, Proc Natl Acad Sci U S A 2008, 105, 8637–8642. [PubMed: 18550842]

[15]. Qin Z, Hu D, Han S, Hong D-P, Fink AL, Biochemistry 2007, 46, 13322–13330. [PubMed: 17963364]

[16]. LeVine H, Protein Sci 1993, 2, 404–410. [PubMed: 8453378]

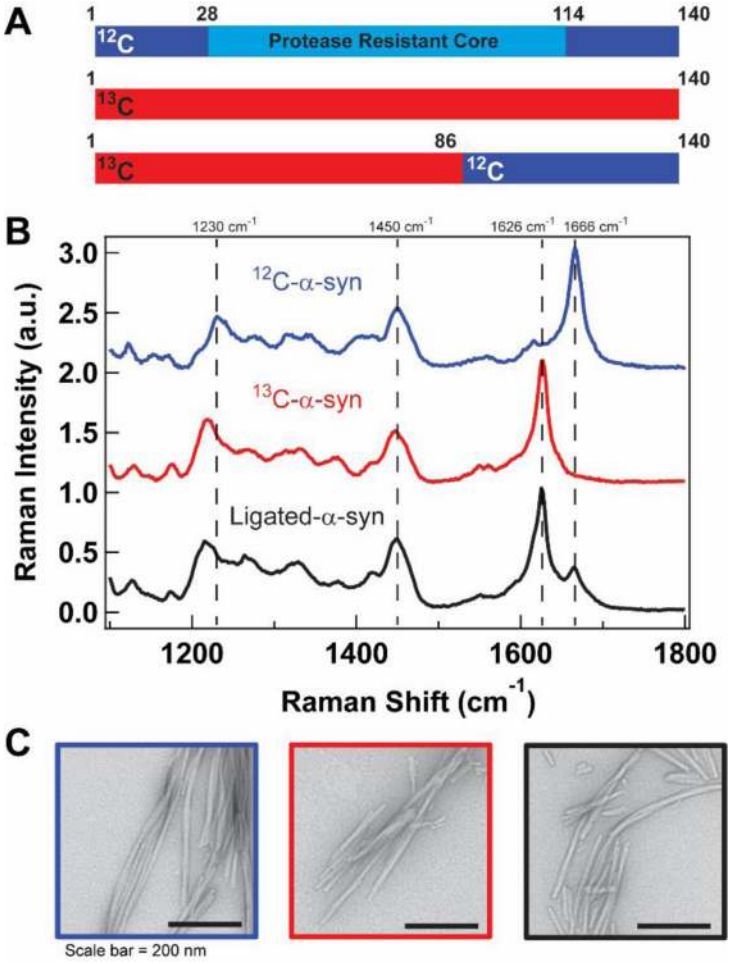

Figure 1.

(A) Schematic representation of the ligated-α-syn construct used in this study. Residues 1–86 and 87–140 are uniformly ^{13}C- (red) and ^{12}C-labeled (blue), respectively. (B) Raman spectra of ^{12}C-α-syn (blue), ^{13}C-α- syn (red), and ligated-α-syn (black). Spectra vertically offset for clarity. (C) Representative negatively-stained TEM images of fibrils formed by α-syn variants. Outline colors correspond to spectra in (B). Scale bar = 200 nm.

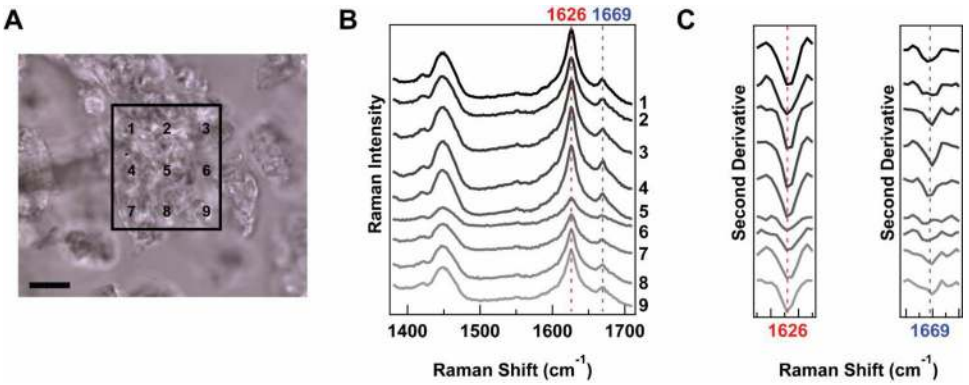

Figure 2.

(A) Bright-field image of ligated-α-syn aggregate probed by Raman microspectroscopy. Raman mapping area is indicated by the black box and the numbers correspond to spatial locations of measurements. Scale bar = 10 μm. (B) Individual Raman spectra collected within a ligated-α-syn aggregate after 5.25 h incubation time. The numbers correspond to locations as indicated in (A). (C) Second-derivative analysis of ^{13}C- and ^{12}C-amide-I bands at 1626 and 1669 cm^{-1}, respectively. Spectra are vertically offset for clarity and dashed lines are drawn for ease of comparison.

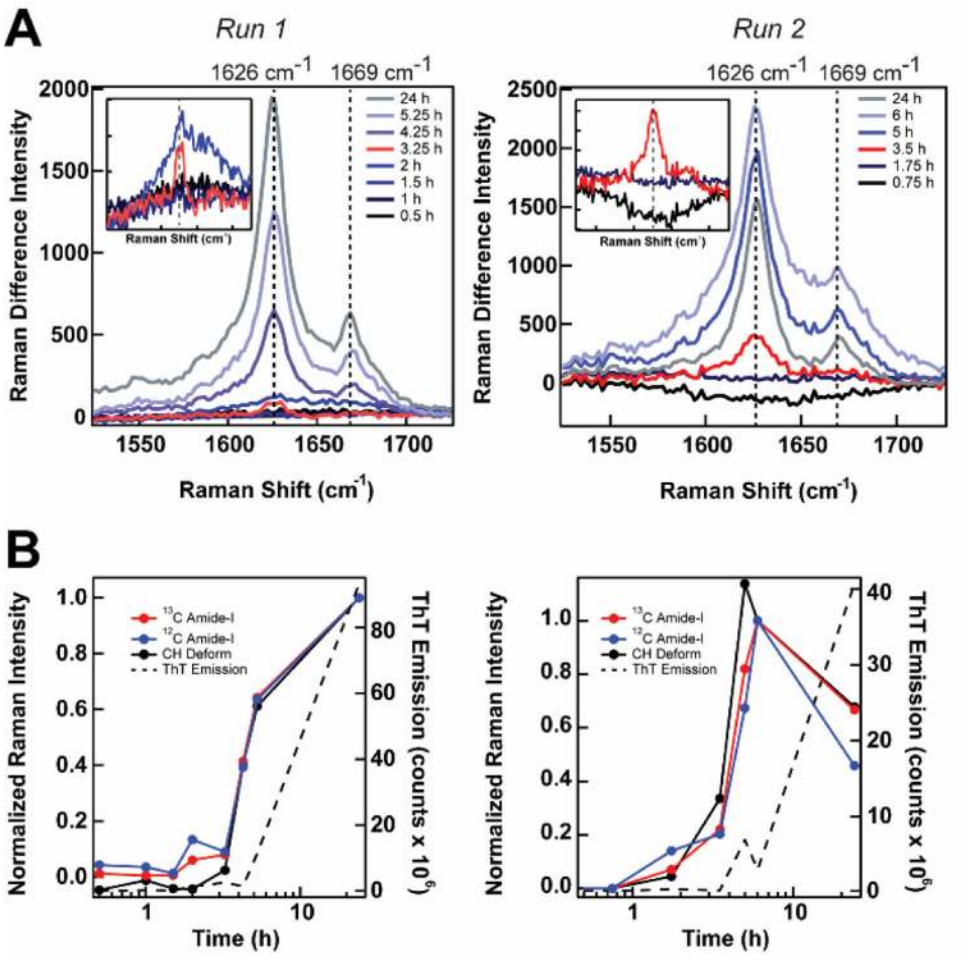

Figure 3.

(A) Raman difference spectra ($t_n - t_0$) of amide-I region for two independent aggregation reactions (left, Run 1; right, Run 2), n = the indicated time point minus initial spectrum at time 0. Early time points are shown in inset for clarity due to large differences in intensity scales. (B) Comparison of ^{13}C-amide-I, ^{12}C-amide-I, C-H deformation (left axis), and ThT emission intensity (right axis) as a function of aggregation time for the two independent aggregation reactions shown in (A). The changes in the Raman peaks have been normalized for comparison.

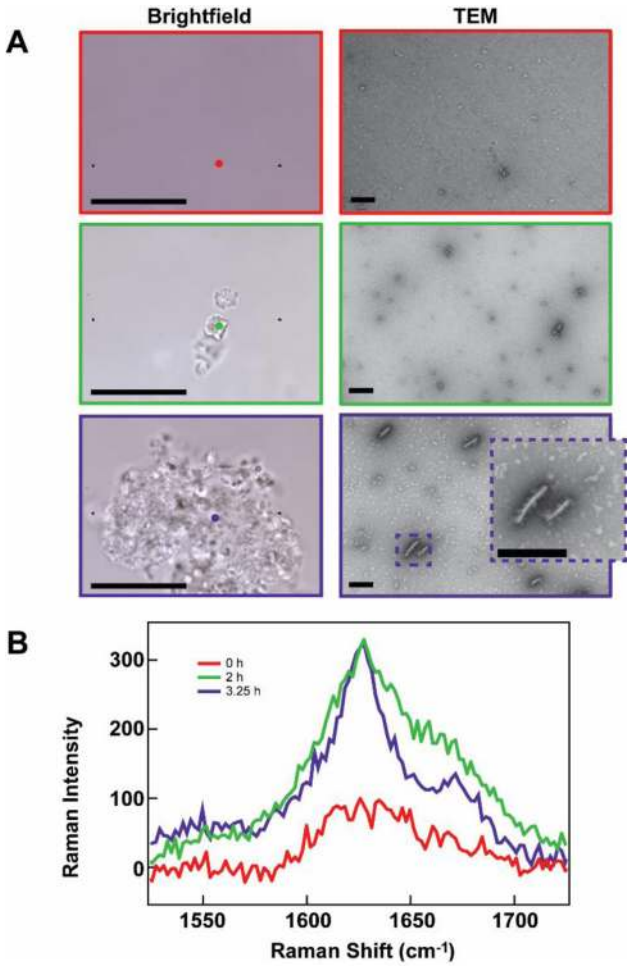

Figure 4.

(A) Representative brightfield (left column) and negatively-stained TEM (right column) images of ligated-α-syn at 0 h (red outline), 2 h (green outline, and 3.25 h (purple outline) for Run 1. Brightfield scale bar = 25 μm, TEM scale bar = 200 nm. (B) Amide-I region of Raman spectra collected at spatial locations indicated by colored dots in brightfield images in (A).